Nano carbon supported platinum catalyst interaction behavior with perfluorosulfonic acid ionomer and their interface structures

Shuang Ma Andersen*

Department of Chemical Engineering, Biotechnology and Environmental Technology, University of Southern Denmark, Niels Bohrs Allé 1, DK-5230 Odense M, Denmark

A B S T R A C T

The interaction between perfluorosulfonic acid ionomer and supported platinum catalyst is essential. It directly influences platinum accessibility, stability of carbon support and platinum, proton conductivity and electron conductivity in an electrode. In this study, we compare the adsorption behavior of Nafion ionomer on platinized carbon nano fibers (CNFs), carbon nano tubes (CNTs) and amorphous carbon (Vulcan). The interaction is affected by the catalyst surface oxygen groups as well as porosity. Comparisons between the carbon supports and platinized equivalents are carried out. It reveals that the platinization step modifies the surface nature of the carbon supports in terms of specific surface area, crystallinity and especially porosity; therefore, ionomer adsorption over carbon is not always representative for the ionomer adsorption over carbon supported catalyst, though indicative. Moreover, the ionomer may have an adsorption preference to the platinum nano particle rather than to the overall catalyst. This was verified by a close examination on the decomposition temperature of the carbon support and the ionomer. The electrochemical stability of the catalyst ionomer composite electrode suggests that the ionomer adsorption on the overall catalyst is a more stable interface structure for fuel cell application.

© 2015 Elsevier B.V. All rights reserved.

1. Introduction

Major challenges prevent proton exchange membrane fuel cells (PEMFCs) from widespread commercialization are: the use of the noble metal platinum as the preferred catalyst on account of its high cost and scarcity [1]; on the cathode side of the fuel cell, the sluggish reaction kinetics for the oxygen reduction reaction (ORR) [1]; and furthermore, PEMFCs suffer from inadequate performance and durability [2]. In order to boost the technology, copious activities are carrying out to explore cheaper [3], more efficient [4] and more durable materials [5]. However, development of any single material is not sufficient. Studies on the interaction and compatibility between the fuel cell components and interface structure are also paramount and can be even more beneficial for the advance of the technology [6,7].

When catalysts are utilized in an electrode, ionomer (such as Nafion) impregnation is routinely applied, which may decrease catalyst loading by several factors [8–10]. In fuel cell reactions, both electrons and protons are involved. The presence of proton conductor in the catalyst layer effectively increases the

proton-electron contact, enlarge the reaction zone, extend the reaction from the surface to the entire electrode; thus, the catalyst utilization in the layer can be dramatically improved. The catalyst layer will in turn generate and sustain a higher current density. One of the generally adapted methods to impregnate Nafion into the electrode is to mix the catalysts, especially supported catalysts, directly with the ionomer, and to use the resulting mixture to fabricate the catalyst layer. The mixing ratio, mixing condition and most important interactions between Nafion ionomer and the catalysts/support (of different surface area, wetting property, and porosity) play a significant role in the performance of the final electrode and cell, as observed by many groups. Sun et al. [11] investigated the morphology, porosity and water uptake of the electrode in relation to the ionomer loading; they concluded that ionomer-catalyst particle interactions control the overall structure of the catalyst layer. Cho et al. [12] studied the effect of cathode structures on the chemical stability of Nafion membranes in terms of hydrogen crossover current density; they observed that structural uniformity of cathodes played the most significant role in the chemical stability of the Nafion membranes. Malek et al. [13] presented systematic mesoscale simulations to study dynamical-structural properties of the catalyst layers in PEFCs with a focus on the effects of applicable solvents with varying dielectric constants, which can be used for the structural design of catalyst layers with optimized

* Corresponding author.
  E-mail address: mashu@kbm.sdu.dk

performance and stability. Yuan et al. [14] illustrated that incorporation of Nafion ionomer with reduced agglomerate size by heat treatment can improve the catalyst performance in DMFC, due to better contact between catalyst particles and the electrolyte. We also observed an optimal catalyst performance under appropriate hot-pressing treatment, which leads to partial melting of the ionomer phase enhancing the component contact [15].

The interaction behavior between the ionomer and the catalyst is individualized. It is generally controlled by the surface property of the adsorbate, on account of identical ionomer morphology. As a new class catalyst support, carbon nano materials, such as carbon nano fiber (CNF) and carbon nano tube (CNT), have gained plenty attention, due to its high stability [16–18] as well as their synergetic effects to assist various reactions [19,20]. They have distinctly difference surface property from the traditional carbons [21–24], such as Vulcan, due to their atomic structure, crystallinity, number of defect, surface oxygen group etc. Moreover, our earlier work [25] carried out on the identical nano carbons has shown that CNTs contain higher amount of surface oxygen groups than CNFs; the surface oxygen groups are significantly increased by acid treatments. Therefore, individual studies on the interaction between the

ionomer and the nano carbon supported platinum catalysts should be carried out.

In the previous work [26,27], we explored the ionomer adsorption behavior on various catalyst supports with systematic treatments. Here, the focus is the interaction between platinized nano carbons and the ionomer. Moreover, the consequent electrode interface structure is investigated according to fuel cell operation conditions based on an accelerated stress test.

2. Experimental

2.1. Sample information

Multi-walled carbon nanotubes (MWCNTs) synthesized by chemical vapour deposition and highly graphitized vapor grown carbon nanofibers were kindly provided by Showa Denko® (Japan) under the trade name VGCF-X™ and VGCF™ respectively. Purification of the carbon nano tube was performed under oxidative condition at 380 °C for 3 h followed by treatment with 5 M hydrochloric acid (AnalytiCals®) at 80 °C for 3 h. The purified product is named as CNT. Afterwards, functionalization of the CNT was
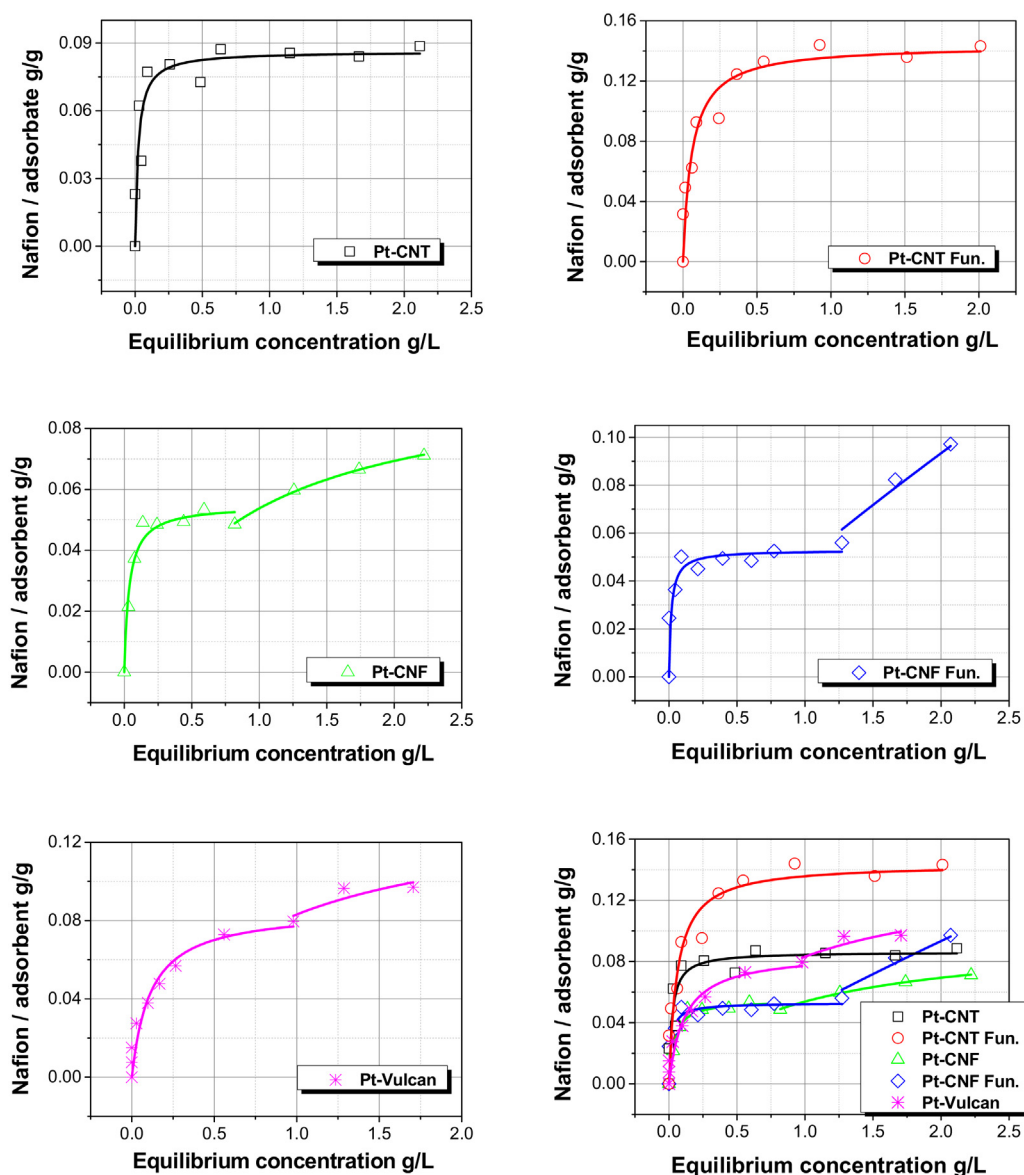

Fig. 1. Nafion ionomer adsorption isotherms for nanocarbon supported platinum catalyst.

carried out in a 1:1 mixture of 2 M HNO_3/1 M H_2SO_4 at 120 °C under refluxing condition for 4 h, and named as CNT Fun. No purification was applied on the carbon fiber, and it is named as CNF. A surface modification is achieved by exposure to mixtures of nitric and sulfuric acid (2 M HNO_3, 4 M H_2SO_4) for 6 h at 120 °C, the corresponding product is named as CNF Fun. Deposition of ~20 wt.% Pt on CNFs was performed by the colloidal polyol method, according to a protocol reported elsewhere [28], which consists the reduction of the H_2PtCl_6 precursor to metallic Pt by ethylene glycol (EG) in alkaline media in the presence of the carbon support.

2.2. Adsorption isotherm studies

A detailed procedure for Nafion ionomer adsorption on different carbon substrates can be found in our previous publications [26,27,29]. Briefly, a thorough mixing/adsorption between catalyst powder and Nafion solution (Sigma–Aldrich) was provided by 15 min ultra-sonication and 24 h mechanical shaking. Then the samples were centrifuged for one hour with 12,000 rmp at 4 °C. Finally 600 μL of well separated clean solution was carefully transferred into a 5 mm NMR glass tube. 20 μL heavy water (Sigma–Aldrich 99.9%) was added to provide a deuterium lock, and 20 μL 1% trifluoroacetic acid (99.9% Aldrich) was added for internal reference. All NMR experiments were performed in a Bruker 400 MHz with an auto-sampler. Signal analysis was done using Mestre Nova®. Data fitting was assisted by OriginPro® 9.1.

2.3. Electrode preparation and electrochemistry

Catalyst ionomer electrodes were prepared by mixing the catalyst powder and 10 wt.% Nafion ionomer in water (Sigma–Aldrich®) and ethanol (1:1) mixture. The final ratio between the Nafion ionomer and the catalyst is around 1:9. For the electrode without the ionomer the solution is 50% ethanol in water. The catalyst suspension was drop coated on a piece of carbon paper (Sigracet® 35DC) of surface area 1 cm² and leave to dry under an IR lamp. A typical electrode contains around 10 μg catalyst (however, the precise loading is extremely difficult to control and therefore only relative change is considered). The electrochemical surface area of the electrodes were evaluated by using static cyclicvoltametry with a sweep rate of 10 mV/s within a voltage range of 0–1.2 V vs. reversible hydrogen electrode (RHE). The electrodes were subjected to the potential cycling between 0.4 and 1.6 V vs. RHE for 2500 cycles with sweep rate of 1 V/s in 1 M H_2SO_4 at room temperature. A carbon rod was used as the counter electrode and a radiometer® Hg/Hg_2SO_4 was used as the reference electrode. Ar purging was maintained during the measurements with a constant flow of 0.2 mL/s. The experiments were carried out with an electrochemical workstation (Zahner® IM6e). The connection between the sample and the device was established with a 0.2 mm thick gold wire.

2.4. Other characterizations

Morphology characterization of the carbon nanomaterials was carried out by Transmission ElectronMicroscopy (TEM) with a Tecnai 12 BioTwin with LaB_6 gun at 120 kV. Brunauer–Emmett–Teller (BET) surface area and porosity measurements were performed by N_2 – adsorption–desorption isotherm at 77 K with Micromeritics® physisorption determination. XRD spectra were performed by Siemens diffractometer D5000 with incidence wavelength 1.5406 Å (Cu Kα). Catalyst powder was ground before XRD measurement and pressed manually into the plastic sample holder. All measurements were conducted at ambient temperature and atmosphere. Spectrum was scanned between 10° and 90°, with steps of 0.02°/s. Peak localization and peak width at half height were identified
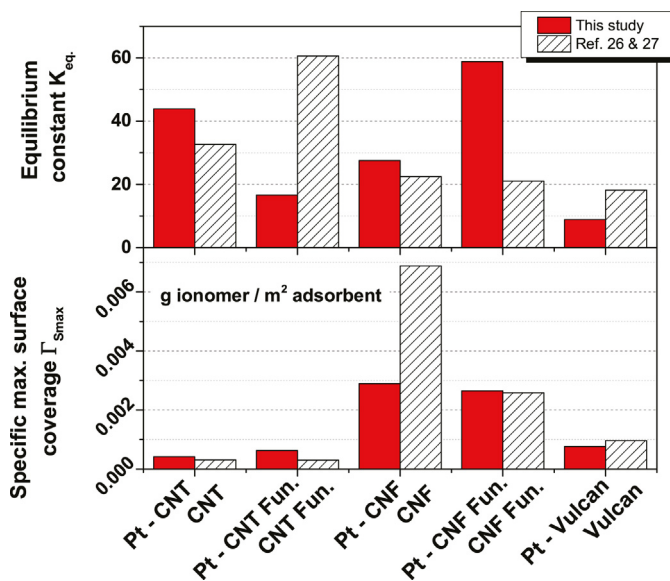

Fig. 2. Adsorption equilibrium constant and specific max. surface coverage of carbon samples with and without platinum nano particles.

with Origin™ 9.1. Platinum crystallite size was calculated using the Scherrer equation [30]. Raman spectroscopy was performed using a Horiba Jobin-Yvon LabRam 300 Raman microscope equipped with a CCD detector and an external cavity stabilized single mode diode laser at 532 nm. Complete thermal decomposition of carbon and ionomer was studied with thermogravimetry using NETZSCH STA 449 F3. In the measurement, about 3–4 mg powder was transferred to an aluminum oxide crucible for TG analysis. The initial and final temperatures are 20 and 900 °C with a heating rate of 20 °C/min. The experiment was performed in a mixed nitrogen and oxygen atmosphere of ratio 4:1, with a total pressure of one atmosphere.

3. Results

3.1. NMR

Nafion ionomer adsorptions on various catalysts were carried out at room temperature. The isotherms are presented in Fig. 1.

Similar to carbon materials, Nafion ionomer adsorption on the platinized carbons can be fairly well described with the Langmuir isotherm. Key parameters including equilibrium constant and specific maximum surface coverage for both platinum catalysts and the non-platinized equivalents are listed in Fig. 2 for easier comparison. The corresponding data are available in supplementary material Table S1. Further explanations will be provided in combination with other information.

3.2. Microscopy

Carbon supported platinum catalysts are closely examined with transmission electron microscopy and the images are shown in Fig. 3. The basic shapes of the support are well maintained after the platinization process. Due to the high surface area of the carbon nano tube, there is relatively low surface coverage by the platinum nano particles. Moreover, platinum aggregation seems more severe for the non-functionalized CNT (Fig. 3a) in comparison to the acid treated equivalent (Fig. 3b). This may indicate that functionalization contributes distribution of the platinum particles. The carbon nano fibers are of much lower surface area in comparison to CNTs. This leads to a high surface coverage of the metal particles in a form of network with slight segregation morphology. The
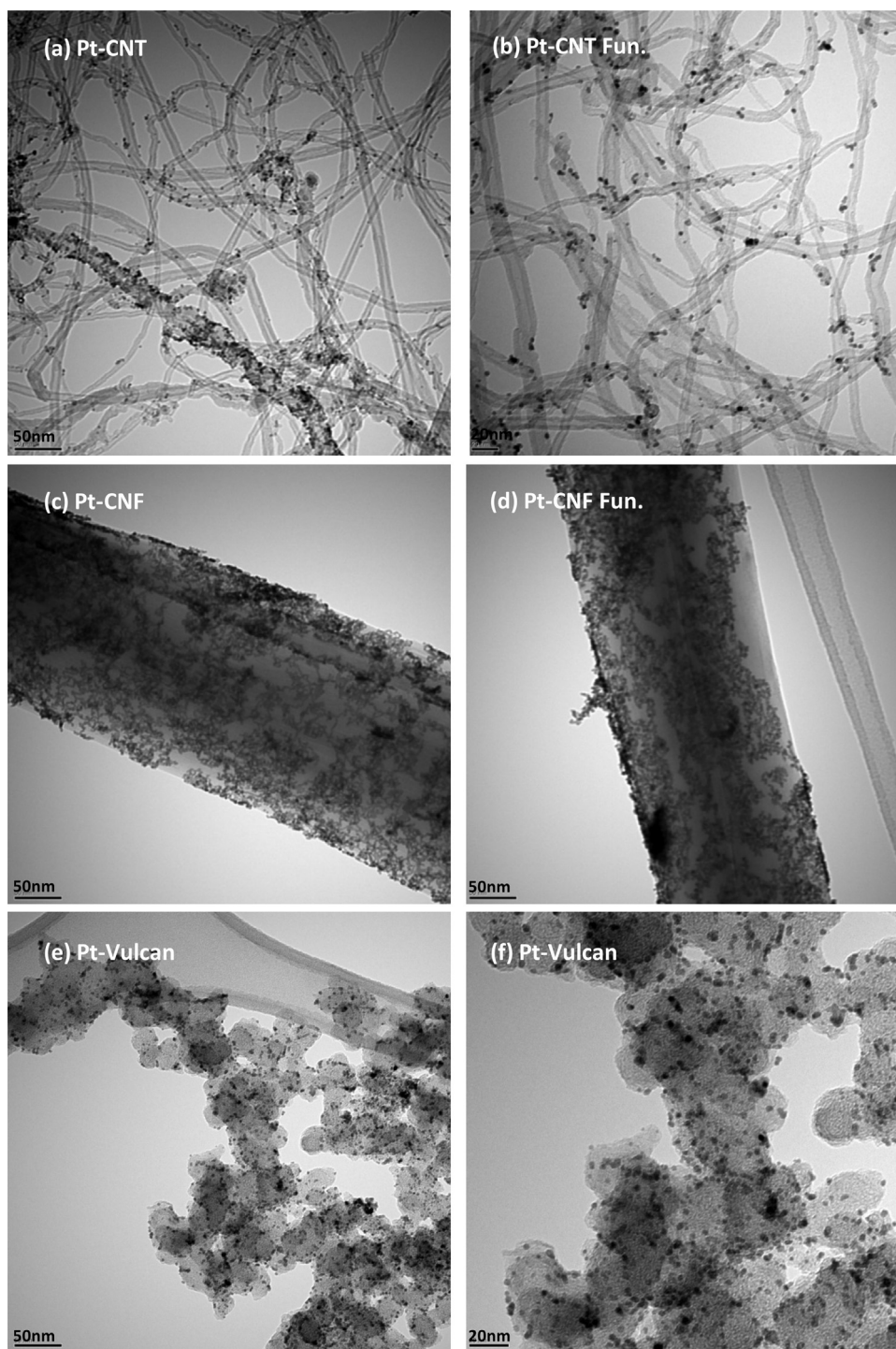
Fig. 3. Transmission electron microscopy on platinized carbons.

Table 1
Sample morphology.

Sample ID	Morphology Brief description	Platinum content[a] %	Platinum diameter[b] nm	Carbon diameter nm
Pt-CNT	Low coverage and catalyst aggregation	20.65	2.29	15, L: 3 μm
Pt-CNT Fun.	Low coverage	16.26	3.25	15, L: 3 μm
Pt-CNF	High cover on the fiber surface	14.83	3.16	150, L: 10 μm
Pt-CNF Fun.	High cover on the fiber surface	19.95	3.46	150, L: 10 μm
Pt-Vulcan	Low coverage decorate the surface	20.86	2.34	~13

[a] The platinum loading was determined with thermogravimetric analysis. Metallic contents in the nanocarbons were corrected.
[b] The platinum diameter is determined based on X-ray diffraction.

platinized products did not show significant differences between pristine (Fig. 3c) and functionalized CNF (Fig. 3d) equivalent, which might be due to the high crystallinity of the virgin form. Platinum on Vulcan appears dark dots decorated spherical amorphous carbon supports. A brief summary is presented in Table 1.

3.3. Surface area and porosity

The specific surface area (SSA) based on BET measurement, meso and micro porosity of the catalysts and the corresponding catalyst supports are presented in Fig. 4. The corresponding nitrogen adsorption-desorption isotherms and extracted data are available in Supplementary material Fig. S1 and Table S2.

Since platinum nano particle of diameter 3 nm has a SSA around 90 m^2/g, addition of the metal particle on the carbon support will lead to a decrease of the SSA for CNTs and Vulcan, and an increase of the SSA for CNFs, as shown in Fig. 4(a).

Based on the meso pore analysis, Fig. 4(b), reduction of the pore area was observed for most samples. The percentage reduction of the meso pore follows an order of Vulcan > CNFs > CNTs. This indicates that formation or location of the platinum nanoparticle significantly change or block the meso pore accessibility for Vulcan and partially CNFs but insignificantly for CNTs. Moreover, functionalized nano carbons show higher reduction of the meso pore. This may imply that the functional groups for platinum anchoring are preferentially situated close to the meso pores.

In general, the microporosity was lost significantly when platinum nano particles were placed on the substrate. Pt-CNT was the only catalyst sample of micro pore left after the platinization.

3.4. XRD

The platinized catalyst was carefully grinded and characterized with XRD. The powder patterns are summarized in Fig. 5.

The diffraction at around $2\theta = 39.6°$, $45.9°$, $67.6°$, $81.70°$ and $86.8°$ can be assigned to the Pt (1 1 1), Pt (2 0 0), Pt (2 2 0), Pt (3 1 1) and Pt (2 2 2). Dominating peaks at approximate $2\theta = 26.6°$, $54.7°$, $77.6°$ and $83.8°$ are due to the diffraction of carbon support. Platinum nano particle size was calculated according to Scherrer formula, and summarized in Table 1. They are between 2.3 and 3.5 nm. The intensity at $2\theta = 26.6°$ indicates crystallinity of the corresponding carbon substrate.

3.5. Raman

Raman spectroscopy was carried out on platinized carbon samples, as shown in Fig. 6.

The intensity ratio between defect band at around 1350 cm^{-1} and graphitic band at 1570 cm^{-1} is used to evaluate crystallinity of the carbon substrate. This corresponds fairly well with the XRD observation. In addition, I_D/I_G values for carbons with and without platinum were summarized in Fig. 7. The corresponding data are available in Supplementary material Table S3. As a general trend, carbon crystallinity was partially compromised after the platinization process.

3.6. Electrochemistry

Cyclicvoltametry and accelerated stress test were carried out on catalyst samples without and with adsorption of Nafion ionomers. Representative CVs are shown in Fig. 8.

Characteristic hydrogen adsorption, desorption (between 0.04 and 0.4 V vs. RHE), platinum oxidation (between 0.8 and 1.2 V vs. RHE) and platinum reduction (between 0.5 and 0.9 V vs. RHE) were easily identified in the electrodes of bare catalysts supported by different nanocarbons, as shown in Fig. 8(a and b). Distinct peaks
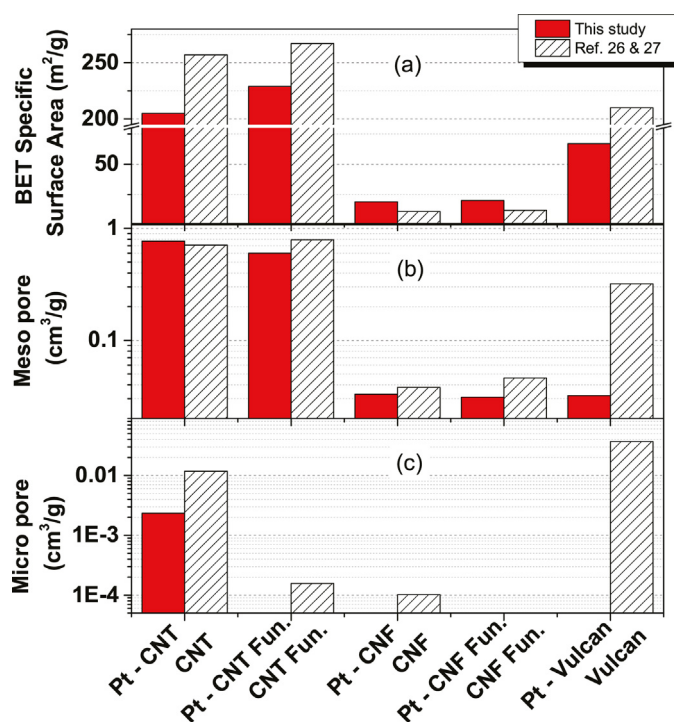

Fig. 4. Surface area and porosity of catalysts and catalyst supports.

of strongly (0.28 V vs. RHE) and weakly (0.12 V vs. RHE) bonded hydrogen [31,32] assigned to Pt (1 0 0) and the combination of Pt (1 1 0) and Pt (1 1 1) crystal faces, were observed. There is an obvious difference in double layer capacity for CNT and CNF based catalysts, which are directly related to the surface area of the supporting carbon.

In the electrodes contain Nafion ionomer, Fig. 8(c and d), both hydrogen adsorption and desorption peaks were found to shift slightly towards lower potential in comparison to the electrodes without the ionomer. This is probably due to the fact that platinum and carbon support are covered with the ionomer (due to their strong affinity [26,27,29], which might affect the hydrogen adsorption. Therefore, a smaller over-potential is required for adsorption and desorption. Furthermore, less distinct peaks for hydrogen adsorption and desorption were observed. This is also caused by the interaction among the components. Depending on the porosity of the support, the location of the catalyst and coverage by the ionomer, the over-potential might shift slightly and the current appears flattened out, as observed in other work [33] as well. Moreover, hydrogen evolution reaction was found to happen easily in the electrodes containing the ionomer. This indicates that Nafion ionomer involved three-phase-boundary can assist releasing of hydrogen molecule from surface adopted proton atoms. This
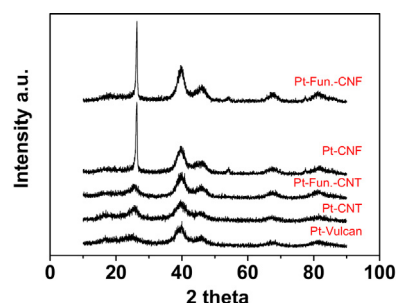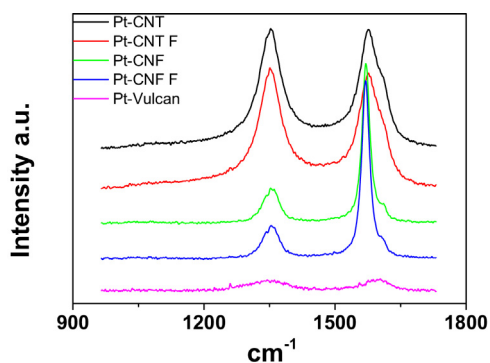

Fig. 5. XRD on platinized carbons.
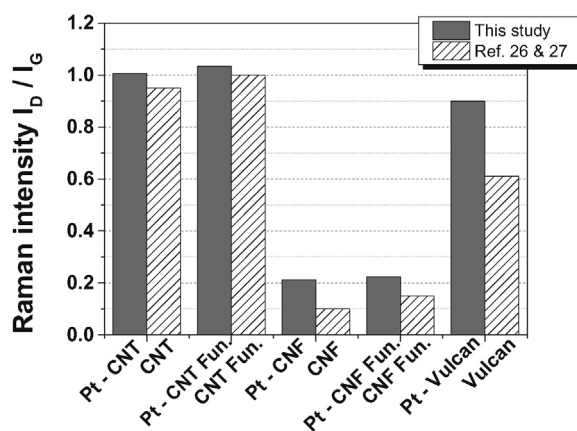
Fig. 6. Raman spectra of platinized carbons.

Fig. 7. Ratio between defective and graphitic carbon.

is probably due to the unique morphology of the ionomer itself or interface structure within the electrode.

Durability of the platinum catalyst was evaluated according to an accelerated stress test protocol. The durability as percentage of the original electrochemical surface area is presented in Fig. 9.

In general, when the ionomer is not involved, CNFs supported catalyst seem relatively more stable than CNTs supported catalyst, which, in turn, is more stable than Vulcan supported catalyst. Catalysts of functionalized support are slightly less durable than un-functionalized equivalents. These are closely related to the crystallinity of the carbon support, since the functionalization partially contributes defects to the carbons structure. Moreover, as an overall observation, participation of Nafion ionomer in the electrode structure extents durability of the catalysts.

3.7. Thermogravimetry

Thermal properties of carbon and polymer component of the electrode were systematically studied by using thermogravimetry. The data are summarized in Fig. 10.

When carbon and carbon supported catalyst are studied, there is only one decomposition peak mainly due to the combustion of carbon with oxygen. When ionomer and carbon or catalyst composites are studied, two decomposition peaks with the ionomer contribution at low temperature and carbon contribution at high temperature.

To systematically study the properties of carbon, the carbon decomposition temperature (CDT) is classified according to the following four systems: (1) naked carbon, (2) carbon ionomer composite, (3) platinized carbon and (4) catalyst ionomer composite for CNTs, CNFs and Vulcan. The data are summarized in the Fig. 11(a).

For each carbon type, the CDT of naked carbon is of the highest value among the four systems. Carbon ionomer composite shows slightly reduced CDT of 2–8%. Reduction of the CDT is probably due to the mixing reduces the chemical potential of the system, which requires less heat for the carbon combustion. Platinum
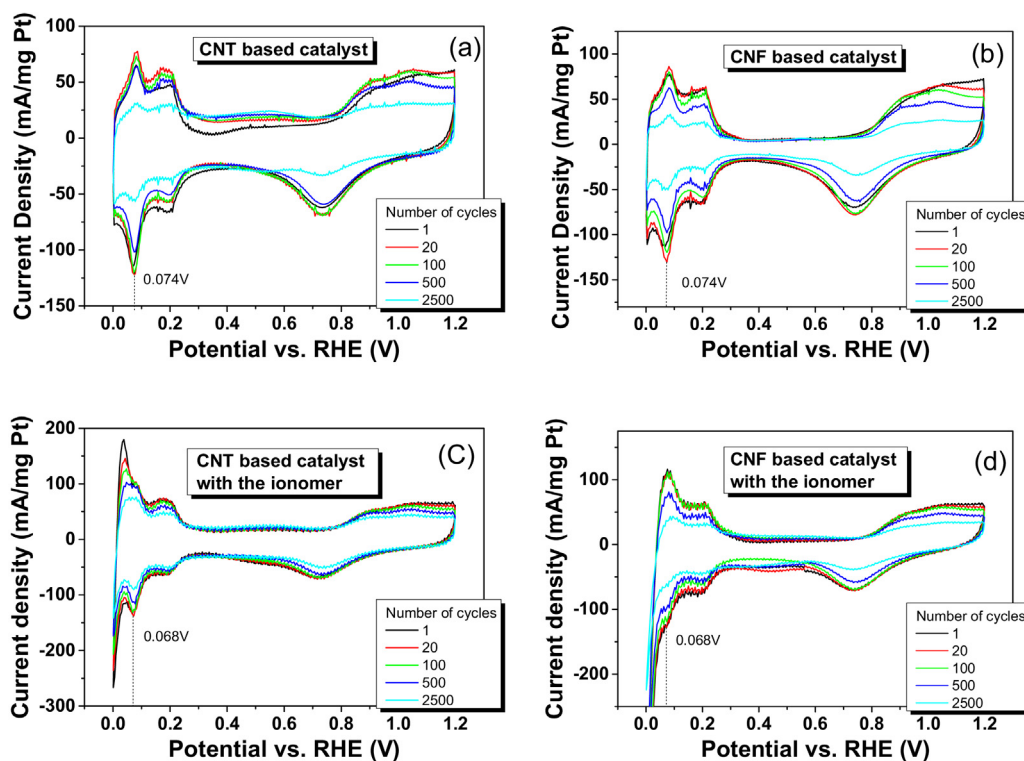

Fig. 8. Representative cyclic voltammograms of platinized nano carbons without (a and b) and with (c and d) Nafion ionomer in the electrode.
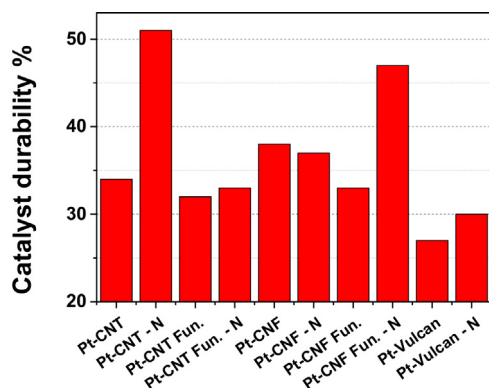
Fig. 9. Electrochemical durability of the catalysts in ionomer catalyst composite electrodes. N denotes Nafion ionomer impregnated.

decorated carbon catalyst shows largely reduced CDT of 20-35%. This is due to the catalytic effect of platinum, which accelerate carbon combustion reaction. Catalyst ionomer composite shows moderately reduced CDT of 18–29%. This is a complex system, where the ionomer has the tendency to partially cover the platinum particle and prevent the metal particle from catalyzing the combustion reaction. In general, the four systems follow the sequence CDT $_{(1)}$ > CDT $_{(2)}$ > CDT $_{(4)}$ > CDT $_{(3)}$.

Similar analysis was also carried out on the ionomer decomposition temperature (IDT), as shown in Fig. 11(b). Decomposition of the ionomer is also catalyzed by the platinum particle; therefore, IDT shows lower value when the catalyst participates. It follows the trend IDT $_{(2)}$ > IDT $_{(4)}$.

4. Discussions

4.1. Ionomer adsorption on the catalysts

As illustrated in Fig. 2, Nafion adsorbs stronger on the platinized CNTs and CNFs, in comparison to platinized Vulcan. This might indicate special affinity between nano carbon supported catalyst and the ionomer, in comparison to amorphous carbon supported catalyst.

The adoption for Pt-CNT has higher equilibrium constant than that of Pt-CNT Fun.'s. This may be largely due to its high meso and micro porosity, as shown in Fig. 4. On the other hand, Pt-CNF has lower equilibrium constant than that of Pt-CNF Fun.'s. This is likely related to the amount of the oxygen group on the surface.

The ionomer shows stronger adsorption on the platinized samples than the equivalent carbons for CNT, CNF and CNF Fun. This might be due to the fact that addition of the platinum nano particle assists the adsorption process. On the other hand, the ionomer shows weaker adsorption on the platinized samples than the equivalent carbons for CNT Fun., and Vulcan. It probably indicates that that addition of the platinum nano particle on the carbon partially blocks the pores, which was originally responsible for the interaction.

Pt-CNFs have higher surface coverage than the catalysts based on Vulcan and CNTs. This is mainly due to their huge porosity difference (Fig. 4). CNT, CNT Fun. and CNF Fun. supported catalysts have higher coverage by the ionomer than their carbon equivalents. CNF and Vulcan supported catalysts show lower coverage than the corresponding carbons. The change of the maximum coverage before and after the platinization may due to factors such as surface roughness, porosity and special interference.
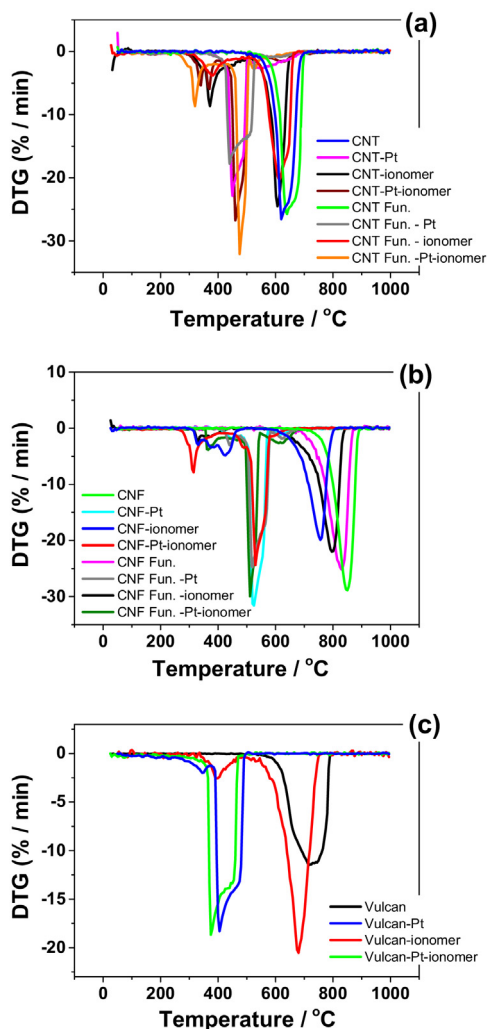

Fig. 10. Thermogravimetry study on carbon and carbon polymer composite.

4.2. Catalyst stability in electrochemical reaction

The participation of the Nafion ionomer in the electrode has shown influence on the durability of the catalyst, as shown in Fig. 9. Moreover, the strength of the interaction between the ionomer and the catalyst (as indicated by the equilibrium constant Keq. from the adsorption study) fits fairly well with the stability of the catalyst, as shown in Fig. 12. This implies that due to the strong interaction, Nafion can effectively interfere with the electrochemical reaction, though the polymer is inert in the process.

Degradation of the catalyst can be generally categorized into the following five aspects: platinum dissolution, Ostwald ripening, coalescence, detachment and support corrosion. Improving the catalyst stability can be carried out on one or all five aspects. This can be realized by a proper interface design.

The function of the Nafion ionomer in the electrode structure, especially interaction with the catalyst has been recently studied [15]. Apart from proton conduction and binder function, the ionomer can improve Pt performance by (1) providing high platinum utilization; (2) decreasing platinum migration and coalescence; (3) reducing carbon corrosion triggered platinum detachment; and (4) influencing transport property of the soluble platinum species which may redeposit. This study reveals that the strength of the ionomer functions is affected by the surface property of the catalyst and the specific interaction behaviors between the catalyst and the ionomer.
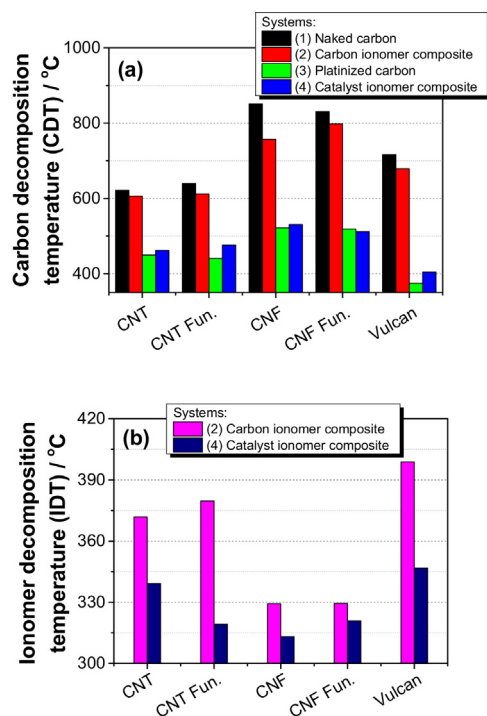
Fig. 11. Decomposition temperature of (a) carbon and (b) ionomer in different systems.
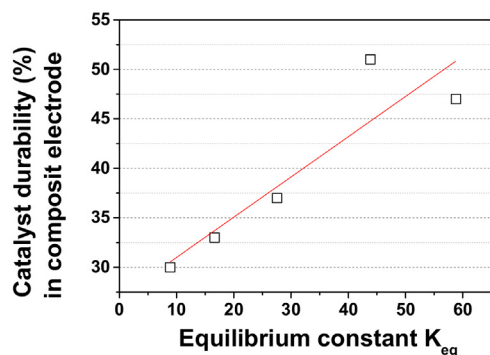

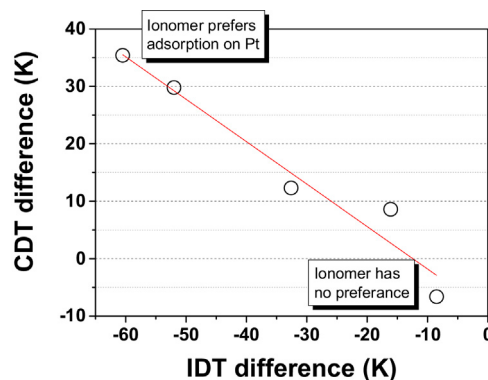Fig. 12. Durability in relation to the adsorption equilibrium constant.

Fig. 13. Differences of the decomposition temperature of ionomer and carbon for catalyst and catalyst ionomer composite.
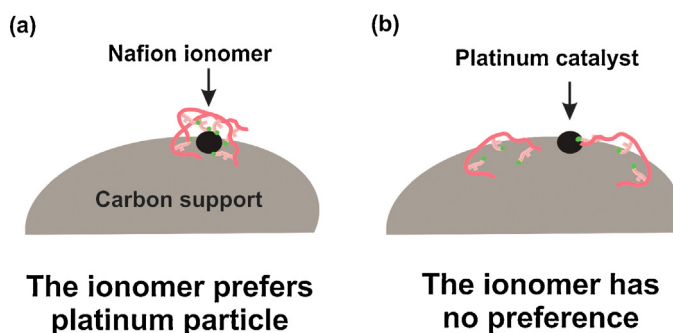

Fig. 14. Ionomer adsorption preferences (a) prefer platinum particle (b) no preference.

4.3. Electrode interface structure

Electrode interface structure brings a direct influence on the stability of the components, as shown in Section 3.6 and 3.7. Especially reflected in the thermal property studies, the differences of the decomposition temperatures between system (2) (platinum supported by carbon) and system (4) (catalyst ionomer composite) can be used to evaluate the adsorption or interface structure of the ionomer and the catalyst. This is based on the fact that surface visibility of the platinum nano particle plays an imperative role in the carbon decomposition. Better the platinum nano particle is covered by the ionomer, higher the decomposition temperature of the carbon will be.

The ionomer may have an adsorption preference on the platinum or the carbon, depending on the surface properties of the adsorbates. When the ionomer favors the platinum, the platinum will be less effective in catalyzing the carbon combustion; there will be a big carbon decomposition temperature (CDT) difference between the catalyst without (system 2) and with (system 4) the

ionomer. On the other hand, when the ionomer has less preference over the platinum particle (equally or more adsorbed over the carbon surface), very little difference will be observed for CDT in the two systems. Similar concept can be applied on the ionomer decomposition temperature (IDT). When the ionomer is preferentially adsorbed on the catalyst, IDT is largely reduced.

The differences of the decomposition temperatures are plotted in Fig. 13. It follows a nice linear regression. This further confirms that ionomer preferences between catalyst or support is reasonable reflected by the comparison of the decomposition temperatures between the two systems. The up left corner of the plot indicates ionomer preferentially adsorbs on the platinum nano particle, as illustrated in Fig. 14(a); this leads to large increase in CDT and large reduction in IDT. The down right corner of the plot (Fig. 13) indicates that the ionomer has no preference over the platinum nano particles or the carbon support, as illustrated in the Fig. 14(b); this lead to only small increase in CDT and small reduction in IDT.

Furthermore, the decomposition temperature of carbon and ionomer are plotted against the equilibrium constant determined by the Langmuir isotherm, as shown in Fig. 15.

Fair linear relationships were observed for both CDT and IDT as function as K_{eq}. This indicates that adsorption strength is related to the ionomer surface coverage preferences. Ionomer coverage on the platinum particle is reflected by the relatively lower equilibrium constant; ionomer coverage on the entire catalyst is reflected by relatively high Keq. values. Since the adsorption equilibrium constant is proportional to the catalyst durability (Fig. 10), the specific adsorption configuration (on the Pt particle or the entire catalyst) is also directly related with the electrochemical performance. This indicates that ionomer coverage on the entire
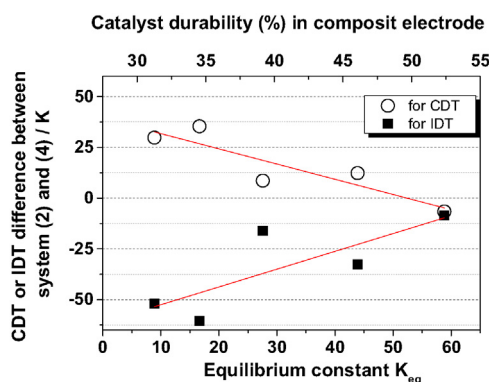
Fig. 15. Interface structure in relation to adsorption property and catalyst stability.

catalyst is a more robust interface structure for that electrochemical application. This may indicate corrosion of the carbon and / or collapse of the interface structure is a more important degradation mechanism. Therefore, more efforts should be placed on optimizing electrode structure and interface improvements.

5. Conclusions

Interaction behavior between Nafion ionomer and various carbon supported (CNTs, CNFs and Vulcan) platinum catalysts was investigated. Strong interaction between the ionomer and the catalyst was observed and it can be described by Langmuir isotherm. The adsorption strength is affected by the surface oxygen group as well as porosity. Due to the fact that platinization can greatly modify the surface property of the carbon support (area, crystallinity and porosity), adsorption between the ionomer and catalyst may be largely different from the adsorption between the ionomer and the support. Therefore, the interaction behavior is highly recommended to be carried out on the platinized samples. The ionomer show stronger interaction with nano carbon supported platinum catalysts than the amorphous carbon. The adsorption strength was found directly related to the electrochemical durability of the catalyst in an ionomer catalyst composite electrode: stronger adsorption between the ionomer and the catalyst, better the durability of the catalyst towards the electrochemical accelerated stress test. This signalizes that interaction between the electrode components is also crucial for stability consideration, which is especially pivotal for the electrode and cell development. Decomposition temperatures of carbon and ionomer reveal that the ionomer coverage on the overall catalyst (rather than on platinum nano particle) is a more stable interface structure for fuel cell application.

Acknowledgements

Appendix A. Supplementary data

Supplementary data associated with this article can be found, in the online version, at http://dx.doi.org/10.1016/j.apcatb.2015. 07.049

References

[1] H.A. Gasteiger, S.S. Kocha, B. Sompalli, F.T. Wagner, Activity benchmarks and requirements for Pt, Pt-alloy, and non-Pt oxygen reduction catalysts for PEMFCs, Appl. Catal. B Environ. 56 (2005) 9–35.

[2] R. Bashyam, P. Zelenay, A class of non-precious metal composite catalysts for fuel cells, Nature 443 (2006) 63–66.

[3] C. You, S. Liao, H. Li, S. Hou, H. Peng, X. Zeng, et al., Uniform nitrogen and sulfur co-doped carbon nanospheres as catalysts for the oxygen reduction reaction, Carbon 69 (2014) 294–301.

[4] N.I. Kim, J.Y. Cheon, J.H. Kim, J. Seong, J.Y. Park, S.H. Joo, K. Kwon, Impact of framework structure of ordered mesoporous carbons on the performance of supported Pt catalysts for oxygen reduction reaction, Carbon 72 (2014) 354–364.

[5] E. Negro, R. Latsuzbaia, M. Dieci, I. Boshuizen, G.J.M. Koper, Pt electrodeposited over carbon nano-networks grown on carbon paper as durable catalyst for PEM fuel cells, Appl. Catal. B Environ. 166-167 (2015) 155–165.

[6] S. Holdcroft, Fuel cell catalyst layers: a polymer science perspective, Chem. Mater. 26 (2014) 381–393.

[7] A. Wang, D.D.L. Chung, Dielectric and electrical conduction behavior of carbon paste electrochemical electrodes, with decoupling of carbon, electrolyte and interface contributions, Carbon 72 (2014) 135–151.

[8] E.A. Ticianelli, C.R. Derouin, A. Redondo, S. Srinivas, Methods to advance technology of proton exchange membrane fuel cells, J. Electrochem. Soc. 135 (1988) 2209–2214.

[9] Wilson MS, Membrane Catalyst Layer for Fuel Cells, U.S. Pat. No. 5,234,777 (1993).

[10] X. Wang, W. Francis Richey, H. Kevin Wujcik, R. Ventura, K. Mattson, A. Yossef Elabd, Effect of polytetrafluoroethylene on ultra-low platinum loaded electrospun/electrosprayed electrodes in proton exchange membrane fuel cells, Electrochim. Acta 139 (2014) 217–224.

[11] C.N. Sun, K.L. More, G.M. Veith, T.A. Zawodzinski, Composition dependence of the pore structure andwater transport of composite catalyst layers for polymer electrolyte fuel cells, J. Electrochem. Soc. 160 (2013) F1000–F1005.

[12] B. Cho, D.A. Langlois, N. Mack, C.M. Johnston, Y.S. Kim, The effect of cathode structures on nafion membrane durability, J. Electrochem. Soc. 161 (2014) F1154–F1162.

[13] K. Malek, M. Eikerling, Q. Wang, T. Navessin, Z. Liu, Self-organization in catalyst layers of polymer electrolyte fuel cells, J. Phys. Chem. C 111 (2007) 13627–13634.

[14] T. Yuan, H. Zhang, A. Zou, S. Khatun, D. Akins, Y. Adam, S. Suarez, A study of the effect of heat-treatment on the morphology of nafion ionomer dispersion for use in the passive direct methanol fuel cell (DMFC), Membranes 2 (2012) 841–854.

[15] S.M. Andersen, A. Dhiman, M.J. Larsen, E. Skou, Importance of electrode hot-pressing conditions for the catalyst performance of proton exchange membrane fuel cells, Appl. Catal. B 172 (2015) 82–90.

[16] H.S. Oh, H. Kim, Efficient synthesis of Pt nanoparticles supported on hydrophobic graphitized carbon Nanofibers for electrocatalysts using noncovalent functionalization, Adv. Funct. Mater. 21 (2011) 3954–3960.

[17] D. Sebastián, A.G. Ruíz, I. Suelves, R. Moliner, M.J. Lázaro, V. Baglio, A. Stassi, A.S. Aricò, Enhanced oxygen reduction activity and durability of Pt catalysts supported on carbon nanofibers, Appl. Catal. B Environ. 115–116 (2012) 269–275.

[18] P. Kolla, C. Lai, S. Mishra, H. Fong, W. Rhine, A. Smirnova, CVD grown CNTs within iron modified and graphitized carbon aerogel as durable oxygen reduction catalysts in acidic medium, Carbon 79 (2014) 518–528.

[19] H. El-Deeb, M. Bron, Microwave-assisted polyol synthesis of PtCu/carbon nanotube catalysts for electrocatalytic oxygen reduction, J. Power Sources 275 (2015) 893–900.

[20] H. Wang, J. Zheng, F. Peng, H. Yu, Pt/IrO2/CNT anode catalyst with high performance for direct methanol fuel cells, Catal. Commun. 33 (2013) 34–37.

[21] P.X. Hou, C. Liu, H.M. Cheng, Purification of carbon nanotubes, Carbon 46 (2008) 2003.

[22] M. Monthioux, B.W. Smith, B. Burteaux, A. Claye, J.E. Fischer, D.E. Luzzi, Sensitivity of single-wall carbon nanotubes to chemical processing: an electron microscopy investigation, Carbon 39 (2001) 1251.

[23] H.S. Oh, K. Kim, Y.J. Ko, H. Kim, Effect of chemical oxidation of CNFs on the electrochemical carbon corrosion in polymer electrolyte membrane fuel cells, Int. J. Hydrogen Energy 35 (2010) 701–708.

[24] D. Sebastián, I. Suelves, E. Pastor, R. Moliner, M.J. Lázaro, The effect of carbon nanofiber properties as support for PtRu nanoparticles on the electrooxidation of alcohols, Appl. Catal. B Environ. 132 (2013) 13–21.

[25] S.N. Stamatin, M. Borghei, S.M. Andersen, S. Veltze, V. Ruiz, E. Kauppinen, E.M. Skou, Influence of different carbon nanostructures on the electrocatalytic activity and stability of Pt supported electrocatalysts, Int. J. Hydrogen Energy 39 (2014) 8215–8224, energy.

[26] S.M. Andersen, M. Borghei, R. Dhiman, H. Jiang, V. Ruiz, E. Kauppinen, E. Skou, Interaction of multi-walled carbon nanotubes with perfluorinated sulfonic acid ionomers and surface treatment studies, Carbon 71 (2014) 218–228.

[27] S.M. Andersen, M. Borghei, R. Dhiman, V. Ruiz, E. Kauppinen, E. Skou, Adsorption behavior of perfluorinated sulfonic acid ionomer on highly graphitized carbon nanofibers and their thermal stabilities, J Phys. Chem. 10 (2014) 814–10823, C, 118.

[28] W. Li, C. Liang, W. Zhou, J. Qiu, Z. Zhou, G. Sun, Q. Xin, Preparation and characterization of multiwalled carbon nanotube-supported platinum for cathode catalysts of direct methanol fuel cells, J. Phys. Chem. B 107 (2003) 6292–6299.

[29] S. Ma, Q. Chen, F. Jøgensen, P. Stein, E. Skou, 19F NMR studies of Nafion™ ionomer adsorption on PEMFC catalysts and supporting carbons, Solid State Ionics 178 (2007) 1568–1575.

[30] A.L. Patterson, The Scherrer Formula for X-Ray Particle Size Determination, Phys. Rev. 56 (1939) 978–982.

[31] B.H. Loo, T.E. Furtak, Intrinsic heterogeneity in the multiple states of adsorbed hydrogen on polycrystalline platinum, Electrochim. Acta 25 (1980) 505–508.

[32] K. Kinoshita, P. Stonehart, Role of platinum morphology on hydrogen adsorption isotherms–IV, Electrochim. Acta 20 (1975) 101–107.

[33] S.M. Andersen, E. Skou, Electrochemical performance and durability of carbon supported Pt catalyst in contact with aqueous and polymeric proton conductors, ACS Appl. Mater. Interfaces 19 (16) (2014) 565–16576.